Fuel 340 (2023) 127549

Contents lists available at ScienceDirect

Fuel

journal homepage: www.elsevier.com/locate/fuel

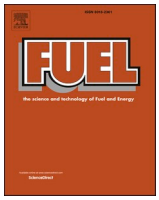

Full Length Article

Process analysis of Pb transformation in the coal devolatilization stage

Guo-chang Song, Wen-ting Xu, Xing-yu Yang, Qiang Song *

Key Laboratory of Thermal Science and Power Engineering of Ministry of Education, Department of Energy and Power Engineering, Tsinghua University, Beijing 100084, China

ARTICLE INFO

Keywords:
Lead
Transformation
Coal
Devolatilization
Process analysis

ABSTRACT

The transformation of Pb during coal devolatilization affects its emission characteristics. Herein, devolatilization experiments were conducted at 1100–1300 °C in a fixed-bed experimental system using four types of coal samples. The occurrences of Pb in coal and devolatilization products were characterized. The release ratio of Pb first increased and then stabilized with time. The Pb release ratio and rate were higher at higher temperatures. Pb in some coal samples was completely released at 1100 °C. Pb in coal was mainly in carbonate- and oxide-bound, sulfide-bound, and residual forms. During devolatilization, carbonate-, oxide-, and sulfide-bound Pb gradually disappeared. Organic-bound and residual Pb first increased and then decreased owing to the conversion of gaseous Pb into Char-Pb by char, according to further form analysis of residual Pb and the experiments of char retaining $PbCl_2$ and PbO. The effects of different volatile components on residual Pb were compared, and H_2S was found to significantly promote the release of residual Pb in coal. The transformation paths of Pb during coal devolatilization were proposed, including the release of original Pb in coal and the reversible conversion between gaseous Pb and Char-Pb. The results help understanding Pb emission and developing control techniques for coal-fired plants.

1. Introduction

Coal combustion is a significant source of atmospheric Pb, which is semi-volatile and may cause serious harm to humans and the environment owing to its toxicity and bioaccumulation [1–3]. Hence, some countries have established the limits for Pb emissions from coal-fired installations [4,5]. After coal combustion, most of the Pb existing in coarse particles is removed by dust removal devices and wet flue gas desulfurization; the remaining Pb in fine particles and gas phase is discharged into the atmosphere with the flue gas [6–8]. Thus, the study of Pb transformation during coal combustion is expected to facilitate the development of corresponding control technologies.

In coal-fired systems, the transformation of Pb is divided into coal combustion and post-combustion stages [9]. In the coal combustion stage, part of the Pb in coal is decomposed and released into the flue gas; the rest is retained in the solid phase owing to thermal stability or reaction with other coal contents [9,10]. As the flue gas is cooled in the post-combustion stage, gaseous Pb in the flue gas migrates to the fly ash particles via chemical reactions in the medium- and high-temperature ranges, as well as through physical adsorption and condensation in the low-temperature range [11–13]. It is important to study Pb transformation in these two stages separately because of significant differences in transformation characteristics and corresponding key influencing factors.

Research on the transformation of Pb during coal combustion has mainly focused on the gas–solid distribution of Pb at the end of combustion [14–17]. The ratio of Pb released into the gas phase varied significantly depending on the experimental method, combustion conditions, and coal type. Wang et al. [16] used four types of coal to perform combustion experiments at 1150 °C and obtained Pb release ratios of 25%–60%, whereas Song et al. [17] conducted combustion experiments on 47 types of coal and found that Pb release ratio at 1100 °C was between 65% and 100%. Under identical combustion conditions, some coal types showed similar Pb release ratios, whereas others exhibited significantly different release ratios, implying that the distribution of Pb in the gas- and solid-phase combustion products is complex.

The transformation of Pb is correlated to the original Pb forms in coal [17,18], which mainly included carbonate- and oxide-bound form (16%–98%), sulfide-bound form (0–52%), and residual form (0–80%) according to Finkelman et al. [19]. Liu et al. [10] performed coal pyrolysis experiments at 1000 °C and found that residual Pb was partially decreased after pyrolysis, whereas Pb in the carbonate-, oxide-, and

* Corresponding author.
E-mail address: qsong@tsinghua.edu.cn (Q. Song).

https://doi.org/10.1016/j.fuel.2023.127549
Received 22 May 2022; Received in revised form 3 January 2023; Accepted 18 January 2023
Available online 26 January 2023

sulfide-bound forms nearly disappeared. Song et al. [17] discovered that Pb only existed as residual form in combustion products of coal at 1100–1300 °C, and its proportion increased for some coals and decreased for others. These studies showed that in a high-temperature environment, some of the Pb forms in coal were released into the gas phase owing to thermal instability, and the rest were transformed into residual Pb in combustion products. The release and conversion ratios of Pb in different forms vary depending on coal types [14–17], which is related to the effect of other components in coal.

Co-combustion experiments of coal and additives proved that some minerals have good Pb retention effect [15,20,21]. Yu et al. [22] reported that kaolin and $PbCl_2$ reacted to produce $PbAl_2Si_2O_8$. Wang et al. [23] found that Al_2O_3, SiO_2, and CaO retained volatile PbO and $PbCl_2$ and generated $PbAl_2O_4$, Ca_2PbO_4, and lead-silicate glass, respectively. Non-mineral components in coal may also affect the transformation of Pb [24]. Huang et al. [25,26] found that HCl promoted the volatilization of Pb during the combustion of solid waste at 850 °C owing to the formation of $PbCl_2$ with high volatility. Chiang et al. [27] suggested that organic Cl (such as PVC) reacted with Pb to form $PbOCl_2$ and PbO_2Cl_2 and promoted Pb release. Zhang et al. [28] hypothesized that SO_2 promoted the conversion of $PbCl_2$ to $PbSO_4$, thereby inhibiting the release of Pb. However, Abdel–Rehim [29] found that $PbSO_4$ decomposed at 1000 °C. Therefore, it is plausible that SO_2 has no effect on the release of Pb during coal combustion at temperatures exceeding 1000 °C. Xu et al. [12] suggested that H_2S promoted the release of Pb from ash at 1000 °C.

These findings suggest that the transformation of Pb during coal combustion is a complex process. Pb distribution in gas–solid combustion products and the change in forms are significantly different owing to different combustion conditions and coal composition. Mastering the transformation mechanism of Pb during coal combustion is important for understanding its transformation behavior and regulating its emissions. Coal combustion can be divided into two stages: devolatilization and char combustion stages [30]. Research on the transformation of other elements (such as alkali metals) during fuel combustion showed that the transformation mechanism of metal elements in the devolatilization stage was different from that in the char combustion stage [31–33]. The transformation of metal elements in the coal devolatilization stage contributes to the gas-phase release of metal elements during the entire combustion process. In addition, the occurrence of metal elements in the devolatilization products affects their transformation in the char combustion stage. However, there have been no reports on the transformation of Pb in different stages.

In this study, four types of coal were used as the raw materials, and a fixed-bed experimental system was used to conduct coal devolatilization experiments with different reaction times at 1100–1300 °C. The dynamic characteristics of Pb release were obtained by measuring the Pb content in coal and devolatilization products. The sequential extraction method was used to analyze the forms of Pb before and after coal devolatilization, and the transformation characteristics of Pb were explored. Co-heating experiments of char with $PbCl_2$ and PbO were conducted to reveal the generation and release mechanism of organic-bound and residual Pb. The effect of volatile components on residual Pb and its mechanism were studied by changing the reaction atmosphere. The transformation paths of Pb in the coal devolatilization stage were established. Based on this work, the effects of maceral groups on Pb transformation, which have not been reported in the past, are worth studying in future researches, since the maceral groups were reported to greatly affect the coal devolatilization and char formation [34–36].

2. Experimental

2.1. Sample

Four types of bituminous coal, which were collected from different power plants in China, were used as raw materials (numbered as #1–4). Before the experiment, coal was ground and sieved to obtain a powder with a particle size of 74–96 μm for later use. The results of the industrial and elemental analyses of the coal samples are summarized in Tables 1 and 2. The contents of Si, Al, Ca, Fe, Mg, Na, and K in the coal samples were determined following the method reported previously [37]. The contents of S and Cl in the coal samples were determined following the national standards of China (GB/T 214–2007 and GB/T 3558–2014, respectively). The methods are introduced in the Supplementary material and the results are presented in Table 3. An inductively coupled plasma emission spectrometer (ICP-OES; Leeman Labs Prodigy7, USA) was used to analyze the Pb content of coal. The ICP-OES results are presented in Table 3. The contents of maceral and mineral groups were determined following the national standard of China (GB/T 8899–2013) and the results are presented in Table S1.

2.2. Experimental setup

Coal devolatilization experiments were performed using a fixed-bed experimental system (Fig. 1). The fixed-bed reactor consisted of an outer tube, support rod, and crucible, all of which were made of corundum. The crucible was attached to the upper end of the rod. The reaction gas was N_2 and its flow rate was set to 500 mL/min, which was controlled using a mass flow controller (D08-1F, China). The reactor was continuously heated in a resistance furnace. When the temperature of the constant-temperature zone reached the set value (1100, 1200, and 1300 °C), the reaction gas was fed from the top of the reactor and discharged through the bottom. After 30 min of continuous ventilation, the temperature and atmosphere in the reactor stabilized. Next, a crucible with 0.8 g of a coal sample was quickly inserted into the reactor. After the set reaction time, the crucible was removed to the bottom. Meanwhile, the feeding of the reaction gas was stopped, and the cooling gas was injected from the bottom. The sample was purged with 2 L/min N_2 and rapidly cooled, after which the solid products were collected for analysis.

2.3. Methods

2.3.1. Devolatization experiments

Devolatilization experiments were conducted with four types of coal as raw materials in the temperature range of 1100–1300 °C. The coal devolatilization gas products mainly included H_2, H_2O, CO_2, CO, and CH_4 [38]. To determine the time required for coal devolatilization, the contents of CO_2, CO, and CH_4 in the devolatilization gas products of the four types of coal at 1100–1300 ℃ were analyzed using a Fourier transform infrared (FTIR) spectroscopy (Thermo Fisher Scientific Nicoiet 6700, USA). The concentration of each component changed synchronously over time. The concentrations of CO_2, CO, and CH_4 in the gas released during coal devolatilization at each temperature were integrated and added over time. When the total amount of the gases released exceeded 95% of the maximum released amount of the aforementioned gases, coal devolatilization was considered complete [31]. This time was selected as the characteristic time for the completion of coal devolatilization at this temperature, as shown in Table 4. The reaction time was set according to Table 4 to obtain the product at the end of coal devolatilization. To obtain a comprehensive understanding of the dynamic characteristics of the Pb transformation, devolatilization experiments with durations of 0.5/1/2/3/5/10 min were also conducted.

Table 1
Proximate analysis of the coal samples (wt.% ad).

Coal	Moisture	Volatile	Ash	Fixed carbon
#1	2.07	28.23	19.98	49.72
#2	0.40	11.07	54.30	34.23
#3	0.77	19.57	35.69	43.97
#4	2.67	33.21	22.86	41.26

Table 2
Ultimate analysis of the coal samples (wt.% daf).

Coal	C	H	N	O
#1	60.73	3.80	1.36	33.70
#2	38.89	2.04	0.65	58.42
#3	50.73	2.99	0.81	45.47
#4	52.19	3.81	0.81	41.57

2.3.2. Calculation of volatile yield and Pb release ratio

The yields of all volatile components were obtained by reducing the quality difference between the reactants and solid products. The coal and solid products, which were removed from the crucible after the reaction, were weighed, and the volatile yield R_{vol} (converted to the mass fraction of raw coal) was calculated according to Equation (1).

$$R_{Vol} = \frac{m_c - m_p}{m_c} \times 100\% \tag{1}$$

where m_c and m_p are the masses (g) of the coal used in the experiment and the residues in the crucible after devolatilization, respectively.

The coal and solid products after the reaction were used to analyze the Pb content and the distribution of Pb forms. The samples were digested as follows [39]. First, 50 mg of the sample was placed in a digestion tank. Then, 10 mL of an aqueous solution of HNO_3 (65%–68%), 1 mL of an aqueous solution of H_2O_2 (30%), and 1 mL of an aqueous solution of HF (30%) were sequentially added to the tank. The tank was placed in a microwave digestion apparatus (Milestone ETHOS UP, Italy) afterwards and was digested at 240 °C for 40 min. The Pb concentration was measured using ICP-OES. The release ratio of Pb (R_{Pb}) during coal devolatilization was calculated using Equation (2).

$$R_{Pb} = \left(1 - \frac{m_p \times c_p}{m_c \times c_c}\right) \times 100\% \tag{2}$$

where c_c and c_p are the Pb contents (μg/g) in the experimental coal and solid products, respectively.

2.3.3. Sequential chemical extraction

The form analysis of Pb in coal and solid products was conducted by modifying the four-step chemical extraction method reported by Finkelman et al. [19,40]. The forms of Pb were divided into five types: water-soluble and ion-exchangeable form (F1), carbonate- and oxide-bound form (F2), sulfide-bound form (F3), organic-bound form (F4), and residual form (F5). The extractants and extraction times used for each extraction step are listed in Table 5. The extraction temperature was 60 °C, which was kept by water bath. The extraction process was described in detail in our previous study [40]. ICP-OES was used to determine the Pb content in the extractant at each extraction step, and the fractions of Pb forms in the coal and char samples were obtained. The fractions of Pb in F1, F2, F3, and F4 ($P_{s,Fj}$, s means "coal" or "char") were calculated using Equation (3). The fraction of Pb in F5 ($P_{s,F5}$) was calculated using Equations (4) and (5).

$$P_{s,Fj} = \frac{M_{s,Fj}}{M_r} \times 100\% \tag{3}$$

$$P_{coal,F_5} = 100\% - \sum_{j=1}^{4} P_{coal,F_j} \tag{4}$$

$$P_{char,F_5} = 100\% - R_{Pb} - \sum_{j=1}^{4} P_{char,F_j} \tag{5}$$

where $M_{s,\ Fj}$ is the amount of Pb (μg) in the F_j form in the coal or char samples, and M_r is the total amount of Pb (μg) in the coal. The recovery rates were 95.3%–101.9% for Pb in coal and 97.6%–104.1% for Pb in char.

2.3.4. Co-heating experiments of char and $PbCl_2$/PbO

The Pb retention effect of char was studied using char prepared by the pyrolysis of fulvic acid at 1100–1300 °C. The char was then mixed with 1% $PbCl_2$ and PbO respectively and heated for 1, 3, 5, or 10 min at 1100–1300 ℃. The Pb content and form distribution of the products were analyzed.

2.3.5. Experiments on the effect of volatile components on residual Pb

To explore the effect of volatile components on residual Pb, the char prepared in #1 coal devolatilization at 1200 °C for 10 min was used as a

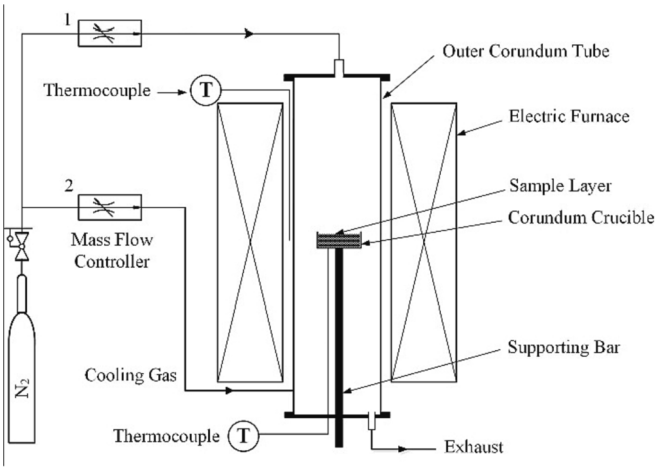

Fig. 1. Schematic of the fixed-bed reactor system.

Table 4
Devolatilization time of coals at 1100–1300 °C (min).

Coal	1100 °C	1200 °C	1300 °C
#1	2.0	1.5	1.2
#2	2.6	2.0	1.3
#3	2.1	1.5	1.0
#4	1.2	1.0	0.5

Table 5
Conditions of sequential chemical extraction.

Form of Pb	Extractants	Time
Water–soluble and ion–exchangeable	1 mol/L CH_3COONH_4	20 min
Carbonate– and oxide–bound	3 mol/L HCl	90 min
Sulfide–bound	2 mol/L HNO_3	40 min
Organic–bound	2 mol/L HNO_3 + 5% H_2O_2	60 min

Table 3
Contents of inorganic components and Pb in coal samples (wt % ad).

Coal	Si	Al	Fe	Ca	Mg	Na	K	S	Cl	Pb ($\times 10^{-4}$)
#1	2.38	5.59	0.42	1.49	0.04	0.01	0.07	0.41	0.055	36.7
#2	14.1	7.74	2.73	0.67	0.34	0.09	1.54	0.33	0.018	138.0
#3	7.68	5.91	1.97	1.32	0.27	0.20	0.51	1.40	0.042	28.1
#4	5.39	2.66	1.86	0.91	0.23	0.13	0.39	1.62	0.043	40.4

carrier of residual Pb. After being placed in the constant-temperature zone of the furnace, different reaction gas components were introduced for a period of time, and then the products were removed to analyze the Pb content. The reaction temperature and time were 1200 °C and 5–20 min, respectively. To study the effects of CO, H_2, CO_2, H_2O, and CH_4 on residual Pb, the pyrolysis experiment of fulvic acid was performed at 1200 °C in another fixed-bed reactor with the same setup, as shown in Fig. 1. The thermal conversion experiment on residual Pb was carried out simultaneously in the fixed-bed reactor, as shown in Fig. 1, when introducing fulvic acid pyrolysis gas, which was used as the carrier of the aforementioned components. In addition, 500 ppm HCl and H_2S were added to the reaction gas (N_2) to study their effects on residual Pb.

3. Results and discussion

3.1. Dynamic characteristics of Pb transformation during coal devolatilization

3.1.1. Dynamic characteristics of Pb release

Fig. 2 shows the curve of the Pb release ratio with reaction time at 1100–1300 °C as well as the volatile yield curve. The release ratios of Pb after 0.5, 1, 2, 3, 5, and 10 min of devolatilization of four types of coal were invetigated. Besides, the Pb release ratios at the characteristic times of each coal devolatilization were also presented in Fig. 2. The release of Pb from the four types of coal first increased rapidly and then tended to level over time. The release rate and ratio of Pb increased with temperature. The maximum Pb release ratios for #1 coal at 1100, 1200, and 1300 °C were 87%, 93% and 100%, respectively. In #2, #3, and #4 coals, the release ratios of Pb were close to or reached 100% after stabilizing at 1100–1300 ℃. This indicates that the thermal stability of Pb in #1 coal was the highest.

Comparison of the Pb release and volatile yield curves in Fig. 2 shows that the change trends of the two were similar, but Pb release significantly lagged behind coal devolatilization. The time at which the Pb release ratio reached 95% of the maximum value was selected as the characteristic time of the completion of Pb release during devolatilization. The characteristic times of completion of Pb release and devolatilization, as well as the corresponding Pb release ratios, are listed in Table 6. It can be seen that the characteristic time of the completion of Pb release is significantly greater than that of devolatilization. However, with an increase in temperature, the characteristic time of completion of Pb release shortened, and the difference between it and the characteristic time of devolatilization was also decreased. At 1300 °C, the characteristic time of Pb release was approximately twice that of devolatilization. The Pb release ratios of different coal types at the characteristic time of the end of devolatilization significantly varied: 42%–72% at 1100 °C with an average value of 58%, 65%–80% at 1200 °C with an average of 74%, and 70%–92% at 1300 °C with an average of 82%. Thus, the release of Pb in the devolatilization stage is a significant contribution to the release of Pb in the overall coal combustion process.

3.1.2. Distribution of solid Pb forms during devolatilization

Fig. 3 shows the distribution of Pb forms in the four types of coal and their solid products produced at 1100–1300 °C and different

Table 6
Characteristic times of coal devolatilization and Pb release and the Pb release ratios R_{Pb} at the corresponding times.

Coal	Temperature (°C)	Pb release		Devolatilization	
		Time (min)	R_{Pb} (%)	Time (min)	R_{Pb} (%)
#1	1100	5.0	87	2.0	60
	1200	3.0	93	1.5	72
	1300	2.0	100	1.2	82
#2	1100	10.0	97	2.6	72
	1200	5.0	99	2.0	79
	1300	2.0	100	1.3	92
#3	1100	10.0	100	2.1	59
	1200	3.0	100	1.5	80
	1300	2.0	100	1.0	85
#4	1100	10.0	100	1.2	42
	1200	5.0	100	1.0	65
	1300	2.0	100	0.5	70

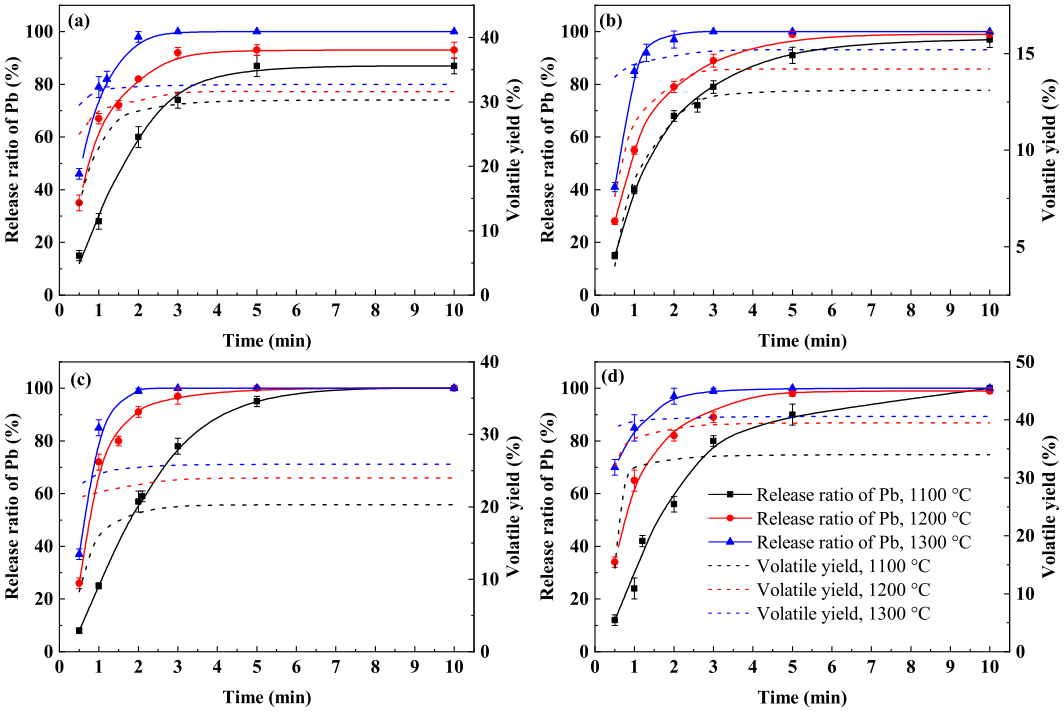

Fig. 2. Release ratios of Pb during coal devolatilization at 1100, 1200, and 1300 °C: (a) #1 coal; (b) #2 coal; (c) #3 coal; (d) #4 coal.

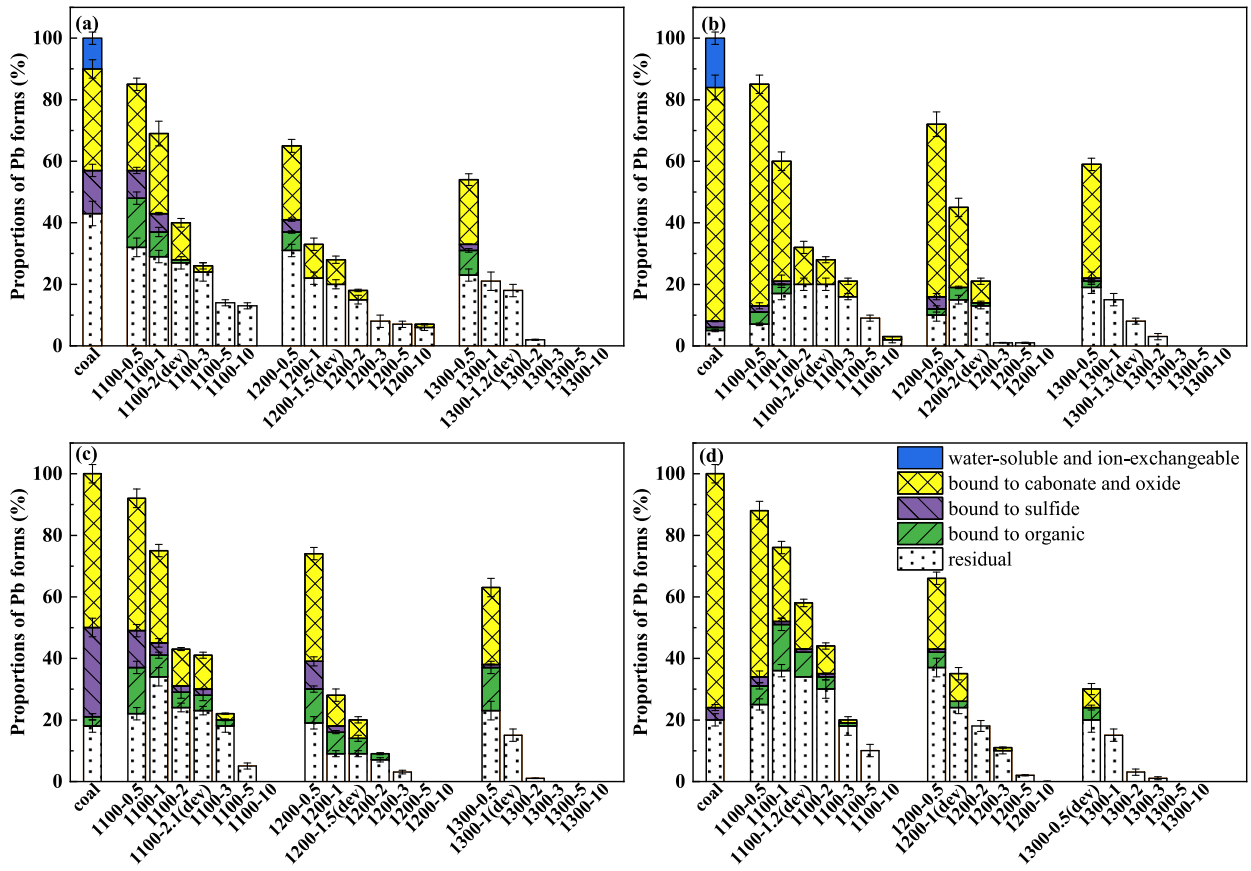

Fig. 3. Distribution of Pb forms in the coal and devolatilization products: (a)#1 coal; (b)#2 coal; (c)#3 coal; (d)#4 coal.

devolatilization times. #1 coal is taken as an example. Pb was mainly present in carbonate- and oxide-bound form (33% of total Pb) and residual form (43% of total Pb). Furthermore, 10% of Pb was in the water-soluble and ion-exchangeable form, and 14% in sulfide-bound form. The distribution of Pb forms in the solid devolatilization products at different temperatures showed similar trends. After devolatilization at 1100 °C for 0.5 min, water-soluble and ion-exchangeable Pb was completely removed from the solid product. Furthermore, the proportions of Pb retained in the solid product as carbonate- and oxide-bound, sulfide-bound, and residual forms were significantly reduced to 28%, 9% and 32% of the total Pb in coal, respectively. Organic-bound Pb was generated in the solid product, accounting for 16% of the total Pb in coal. With increasing reaction time, the proportion of Pb retained in the solid products decreased for all forms. The sulfide- and organic-bound Pb disappeared after 2 min. The carbonate- and oxide-bound Pb were removed after 3 min. The proportion of residual Pb decreased to 14% of the total Pb at 5 min and then did not change over time. At 1200 °C, the proportions of carbonate- and oxide-bound Pb, as well as sulfide-bound Pb in the solid products decreased continuously and basically disappeared at 2 and 1 min, respectively. The proportion of Pb retained in solid products in residual form also decreased continuously but stabilized after 3 min at approximately 7% of the total Pb. Organic-bound Pb in the solid products was formed at 0.5 min, accounting for 6% of the total Pb, but disappeared completely at 1 min. At 1300 °C, the proportions of carbonate- and oxide-bound and sulfide-bound Pb in the solid products decreased to zero after 1 min. The proportion of organic-bound Pb increased to 8% of the total Pb at 0.5 min but disappeared completely at 1 min. Residual Pb in the solid products disappeared after 2 min.

The distribution of Pb forms in the solid products produced at different temperatures corresponding to the characteristic time of devolatilization completion was investigated. At 1100 °C, the proportion of residual Pb was the highest, accounting for 27% of the total Pb, and that of the carbonate- and oxide-bound forms was 12%. At 1200 °C, the proportions of residual Pb and carbonate- and oxide-bound Pb were 20% and 8% of the total Pb, respectively. At 1300 °C, Pb was present only in the residual form, accounting for 18% of the total Pb. After the devolatilization of coal was completed, less than half of Pb remained in solid products, where it mainly existed in the residual form. With an increase in temperature, the proportion of Pb retained in solid products to total Pb in coal decreased.

The changes in the Pb form distribution during the devolatilization of #2, #3, and #4 coals were similar to those of #1 coal. In #2 coal, Pb mainly existed in carbonate- and oxide-bound form, which accounted for 76% of the total Pb in coal; 16% of Pb were in the water-soluble and ion-exchangeable form and 5% in the residual form, respectively. In #3 coal, Pb was mainly in carbonate- and oxide-bound form (50%), sulfide-bound form (29%), and residual form (18%). In # 4 coal, Pb mainly existed in carbonate- and oxide-bound form (76%) and residual form (20%). During the devolatilization of #2, #3, and #4 coals, the distribution of Pb forms retained in the solid products showed similar characteristics to that in #1 coal: (1) the proportions of carbonate- and oxide-bound and sulfide-bound Pb to total Pb in coal decreased to 0 over time; (2) the proportion of organic-bound Pb to total Pb in coal first increased and then decreased to 0; (3) in the solid products generated at the characteristic time of devolatilization completion, residual Pb accounted for the highest proportion of total Pb in coal; (4) with the increase in temperature, the time at which the proportion of organic-bound Pb to total Pb in coal increased to the peak or each form of Pb completely disappeared shortened. It should be pointed out that in contrast to the #1 coal, the residual Pb in the solid products first increased and then decreased to 0 during the devolatilization of #2, #3, and #4 coals. For instance, in the devolatilization of #2 coal at 1100 °C, the proportion of residual Pb in the solid products to total Pb in coal

increased from 5% to 20% within 2 min, then decreased continuously and disappeared at 10 min.

In summary, Pb in the four types of coal was mainly in carbonate- and oxide-bound, sulfide-bound, and residual forms. Small amounts of water-soluble and ion-exchangeable as well as organic-bound Pb were also detected in some coals. During coal devolatilization, water-soluble and ion-exchangeable, carbonate- and oxide-bound, and sulfide-bound Pb decreased and finally disappeared with time; the rate of decrease was accelerated by increasing temperature. The organic-bound Pb first increased and then decreased to zero over time. Residual Pb decreased monotonically with devolatilization time for #1 coal but first increased and then decreased to 0 for #2, #3, and #4 coals. All forms of Pb in coal were thermally unstable and released. In the order of thermal stability from weak to strong, Pb forms are arranged as follows: water-soluble and ion-exchangeable Pb < sulfide-bound Pb < carbonate- and oxide-bound Pb < organic-bound Pb < residual Pb. In addition, the phenomenon that organic-bound Pb and residual Pb first increased and then decreased during coal devolatilization indicated that transformation between different forms of Pb occurred, which is discussed in Section 3.1.3.

3.1.3. Analysis of transformation between different forms of Pb during devolatilization

During the devolatilization of the four types of coal, the proportions of organic-bound Pb in the solid products to total Pb in coal first increased and then decreased to zero. The proportions of residual Pb in the solid devolatilization products of #2, #3, and #4 coals also first increased and then decreased to zero. This indicates the conversion of other forms of Pb to organic-bound and residual Pb. However, with the extension of the reaction time, the organic-bound and residual Pb in #2, #3, and #4 coals disappeared, indicating that the conversion products were thermally unstable and were completely released at 1100 °C.

Organic-bound Pb accounted for a small proportion of the original Pb in the experimental coal, which can be ignored. However, organic-bound Pb was newly generated during coal devolatilization, which was probably because of the retention of gaseous Pb by the char generated from coal devolatilization. The mechanism of interaction between char and Pb has not yet been reported. Zhao et al. [31] found that inorganic K was transformed into organic K through the reaction with char during biomass pyrolysis. Pb may also exhibit a similar behavior during coal devolatilization; that is, inorganic Pb is released into the gas phase and retained as organic-bound Pb by char. The organic-bound Pb gradually decreased to 0 in the later stage of devolatilization, indicating that it was thermally unstable and that the reaction between gaseous Pb and char was reversible. During the initial stage of devolatilization, the concentration of gaseous Pb in the sample layer was high, and gaseous Pb probably migrated into the char. At the later stage of devolatilization, organic-bound Pb was decomposed and released owing to the reduction in Pb release and low gaseous Pb concentration. This hypothesis is verified in Section 3.2.1.

The formation of residual Pb during coal devolatilization may be attributed to the retention of Pb in insoluble aluminosilicate by Si and Al in coal [22,41]; this form of Pb is referred to as Als-Pb in this study. As reported in the study on K transformation during biomass pyrolysis, part of the Char-K retained by char was acid-insoluble [42]. Therefore, another path for the generation of residual Pb was proposed; that is, part of the Pb probably reacted with char to form insoluble Char-Pb, which is referred to as insol-Char-Pb in this study. Als-Pb and insol-Char-Pb did not dissolve in nitric acid or hydrogen peroxide at room temperature. They were classified as the residual form when analyzed by sequential chemical extraction. In this study, different digestion methods (HF-containing and HF-free digestion systems) were used to treat coal and devolatilization solid products to further identify insol-Char Pb and Als-Pb in residual Pb.

First, four types of coal and their solid devolatilization products obtained at 1200 °C and 0.5 min were analyzed. Table 7 lists the results of the Pb content analysis using different digestion and extraction methods. The total Pb content in the sample, w_1 (μg/g), was measured by microwave digestion with $HNO_3 + H_2O_2 + HF$. The measured Pb content when digesting with $HNO_3 + H_2O_2$ under the same conditions is denoted as w_2 (μg/g). At room temperature, the sum of the extractable Pb content using the extractants shown in Table 4 is denoted as w_3 (μg/g). The residual Pb content determined using the sequential chemical extraction method was found as (w_1–w_3). For coal, $w_2 \approx w_3$ indicated that residual Pb in coal was dissolved only in the microwave digestion system containing HF and that this part of the Pb was Als-Pb. In the solid product char, $w_2 > w_3$, indicating that the residual Pb in the char was composed of two parts: Als-Pb and insol-Char Pb, which could not be extracted at room temperature but was dissolved with $HNO_3 + H_2O_2$ at high temperature and pressure, with content of (w_2–w_3). Using this method, the residual Pb in the solid devolatilization products under other working conditions was further divided into insol-Char Pb and Als-Pb, and the changes in their contents were analyzed.

[a]"w_1" is the total Pb content in the sample measured by microwave digestion with $HNO_3 + H_2O_2 + HF$. [b]"w_2" is measured by digestion with $HNO_3 + H_2O_2$. [c]"w_3" is the sum of the extractable Pb content using the extractants shown in Table 4.

Fig. 4 shows the proportions of insol-Char-Pb and Als-Pb to the total Pb in coal at different temperatures and reaction times. During the devolatilization of the four types of coal, the content of insol-Char-Pb in the solid products first increased and then gradually decreased to zero with time. This change was similar to that of organic-bound Pb. In the early stage of devolatilization, part of the Pb released into the gas phase was retained by the char to form insol-Char-Pb. Insol-Char-Pb was thermally unstable and decomposed and released because of the low concentration of gaseous Pb in the sample layer during the later stages of devolatilization. The change trends of Als-Pb in the solid devolatilization products of #2, #3, and #4 coals were similar; that is, Als-Pb content rapidly decreased to zero with time. The higher the temperature, the faster was the decline. In the solid devolatilization products of #1 coal, the proportion of Als-Pb to total Pb in coal also decreased with time, but 13% and 7% of Als-Pb remained stable at 1100 and 1200 °C, respectively; however, Als-Pb disappeared entirely at 1300 °C. Combined with the characteristic time of devolatilization completion in Table 4, this shows that Als-Pb reached stability or was completely released at the end of devolatilization. There are two possible release mechanisms of Als-Pb: (1) decomposition and release owing to its thermal instability and (2) release through the action of other components in coal [12]. Some Als-Pb was still present in solid products after devolatilization of #1 coal, indicating that it was stable in the high-temperature environment, and the release of this part of Pb occurred more likely because of the action of other components in coal. Changes in the Als-Pb content also showed that Pb was not retained in the solid phase by aluminosilicate during coal devolatilization. The increase in residual Pb was attributed to the retention of gaseous Pb by the char.

In conclusion, during coal devolatilization, the original water-soluble and ion-exchangeable, carbonate- and oxide-bound, and sulfide-bound Pb in coal was completely released owing to thermal instability. The original residual Pb in coal was Als-Pb, which was also released. The Als-Pb in #2, #3, and #4 coals was completely released at

Table 7
Pb contents in coal and char samples determined by different methods. (μg/g).

Sample		w_1^a	w_2^b	w_3^c
coal	#1	36.7	20.2	20.9
	#2	138.0	132.6	131.1
	#3	28.1	19.4	19.9
	#4	40.4	32.1	31.5
1200 °C-0.5 min char	#1	31.8	26.3	21.4
	#2	107.6	92.2	72.2
	#3	26.4	23.4	19.6
	#4	45.4	40.9	19.9

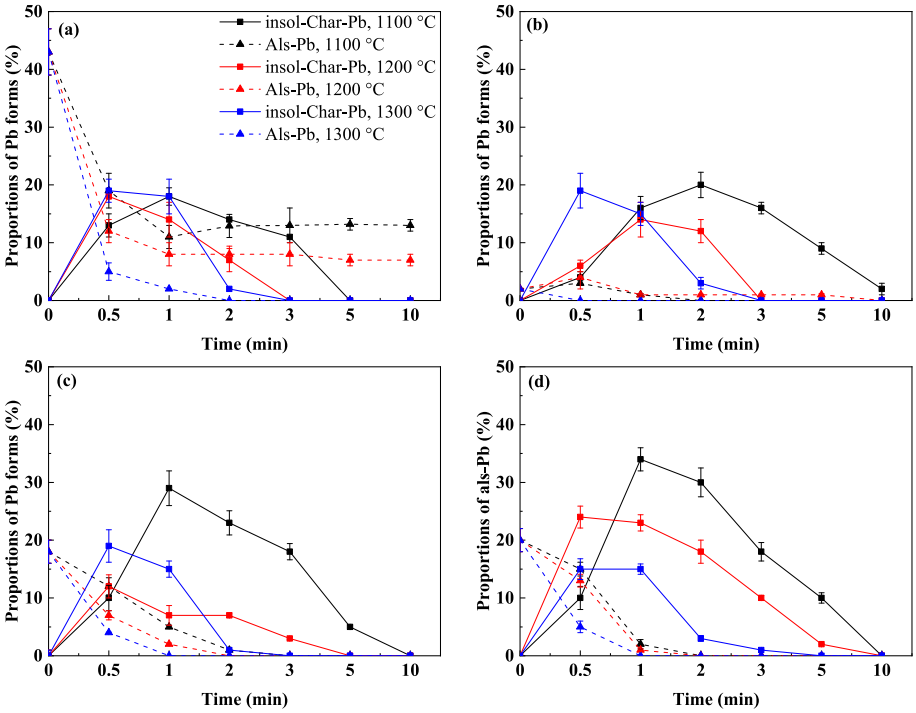

Fig. 4. Proportions of insol-Char-Pb and Als-Pb during coal devolatilization: (a)#1 coal; (b)#2 coal; (c)#3 coal; (d)#4 coal.

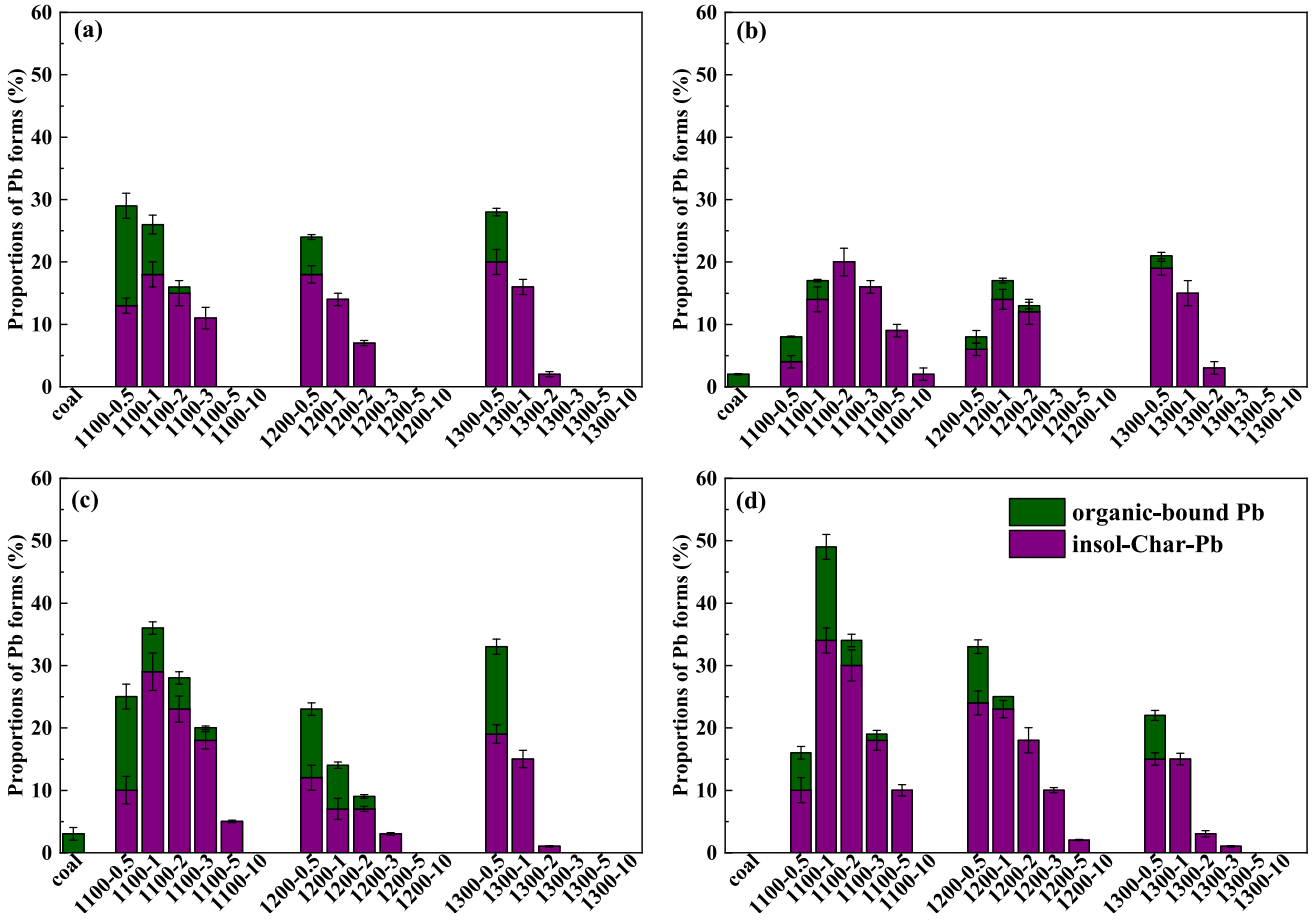

Fig. 5. Proportions of organic-bound Pb and insol-Char-Pb during coal devolatilization: (a)#1 coal; (b)#2 coal; (c)#3 coal; (d)#4 coal.

the experimental temperature. Conversion between different forms of Pb occurred, mainly through the interaction between gaseous Pb and char to generate Char-Pb. According to the sequential extraction results, the generated Char-Pb consisted of organic-bound Pb, which could be extracted by $HNO_3 + H_2O_2$, and residual Pb, which was insoluble in $HNO_3 + H_2O_2$, resulting in an increasing proportion of organic-bound Pb and residual Pb (insol-Char-Pb) in the solid products of devolatilization. However, owing to thermal instability, Char-Pb completely decomposed and was released when the concentration of gaseous Pb was low in the surrounding environment. The mechanism of Pb retaining by char and the release mechanism of residual Pb are explored in detail in Section 3.2.

3.2. Analysis of the mechanism of Pb transformation during coal devolatilization

3.2.1. Generation and release of Char-Pb

Fig. 5 shows the dynamic changes in the proportion of insol-Char-Pb and organic-bound Pb to total Pb in coal during devolatilization. The sum of the two forms of Pb represents the proportion of Char-Pb to total Pb in coal. During devolatilization of different coals at different temperatures, Char-Pb first rapidly increased and then gradually decreased to zero. The proportion of Char-Pb generated by #4 coal at 1100 °C for 1 min was the highest, reaching 49% of the total Pb in coal. The higher the temperature, the faster the ratio of Char-Pb to total Pb in coal reached its peak and declined to zero, indicating that the conversion rate was accelerated. The peak value of the proportion of Char-Pb to total Pb in coal showed no clear trends with temperature. As the temperature increased, the proportion of Char-Pb to total Pb in coal first increased and then decreased during the devolatilization of #1 and #3 coal, increased continuously for #2 coal, and decreased continuously for #4 coal. The Char-Pb generated in the solid products was mainly insol-Char-Pb. With an increase in temperature, the proportion of insol-Char-Pb in Char-Pb increased. For example, the proportions of insol-Char-Pb in the total char Pb in the solid devolatilization products of #1, #2, #3, and #4 coals at 1300 ℃ for 0.5 min were 71%, 91%, 58% and 68%, respectively. Organic-bound Pb was only dominant in #3 coal treated at 1100 °C for 0.5 min. The changes in the amount and form distribution of Char-Pb are probably related to the amount and morphology of gaseous Pb released during coal devolatilization. The maceral groups in coal can affect the properties of the char, such as internal surface area, and then affect the generation of Char-Pb [36].

Owing to the extremely low concentration of Pb in coal and devolatilization products, it was impossible to directly characterize its content and form. Thermodynamic equilibrium calculation results [16] showed that at 1100–1300 °C, the main form of Pb in the gas phase was PbO. When the Cl content in the coal was high, more Pb was present in the form of $PbCl_2$ [43–45]. Considering that fulvic acid is a common type of organic matter in coal [46], fulvic acid pyrolysis was used to simulate the generation of char during coal devolatilization. The char prepared from fulvic acid was mixed with 1% $PbCl_2$ and PbO respectively and then heated at 1100–1300 °C in an inert atmosphere. The Pb content and distribution of Pb forms in the solid products were analyzed at different heating times. The results are shown in Fig. 6. The change in the amount and form distribution of Pb was similar to that shown in Fig. 5: the amount of retained Pb initially rapidly increased with time but then gradually decreased until complete removal. The conversion rate increased with increasing temperature. Pb was retained in two forms: organic-bound Pb and insol-Char-Pb. The thermal stability of organic-bound Pb was worse, and it was eliminated earlier than insol-Char-Pb. There was little difference between the retention amounts of $PbCl_2$ and PbO. The proportion of organic-bound Pb in the $PbCl_2$ retention products was higher than that in the PbO retention products. This shows that during coal devolatilization, the higher the proportion of $PbCl_2$ in the released Pb, the easier it was for organic-bound Pb to form. The form of Pb in the gas phase was significantly affected by the presence of Cl. The Cl content in #2 coal was lower than that in the other three types of coal; hence, Pb was more easily released to the gas phase in the form of PbO and then retained as insol-Char-Pb.

3.2.2. Release of Als-Pb

The original residual Pb in the coal existed in the form of combination with silicoaluminate. During coal devolatilization, Als-Pb was released. Its release dynamics varied with coal type and temperature. Als-Pb in #2, #3, and #4 coals was completely released at 1100 °C. In #1 coal, 13% and 7% of Als-Pb were stable in the solid phase at 1100 and 1200 °C, respectively, and Als-Pb was completely released only at 1300 °C. To determine the reason for this difference, the solid product of #1 coal devolatilization (1200 °C, 10 min) was used as the carrier of Als-Pb, and the effects of different volatile components on Als-Pb were compared by changing the composition of the reaction gas.

The volatiles released from coal mainly included CO, H_2, CO_2, H_2O, CH_4, etc. [47]. The generated HCl and H_2S may also affect the release of Pb [12,48]. Fulvic acid is composed of C, H, and O, and its pyrolysis gas includes CO, H_2, CO_2, H_2O, and CH_4. As shown in Fig. 7, these components had no effect on the release of Als-Pb from the char. When 500 ppm HCl was continuously injected for 5 min, 34% of Als-Pb was released. Extension of the reaction time did not affect the release ratio of Als-Pb. When 500 ppm H_2S was continuously introduced for 5 min, the release ratio of Als-Pb was 83%, which was 2.4 times that at the same concentration of HCl. With the extension of the reaction time to 10 min, Als-Pb was completely released. H_2S and HCl are both favorable for the release of Pb owing to the formation of PbS and $PbCl_2$ with high volatility [12,25]. The results point to the higher reaction activity of H_2S with Als-Pb than HCl. Considering that the amount of H_2S released during coal devolatilization is higher than that of HCl [49], H_2S is considered to be the main factor leading to the release of Als-Pb.

The changes in H_2S concentration in the gas-phase products during the devolatilization of the four types of coal were obtained from FTIR spectra, and the results are shown in Fig. 8. Figure 4 and 8 show that the

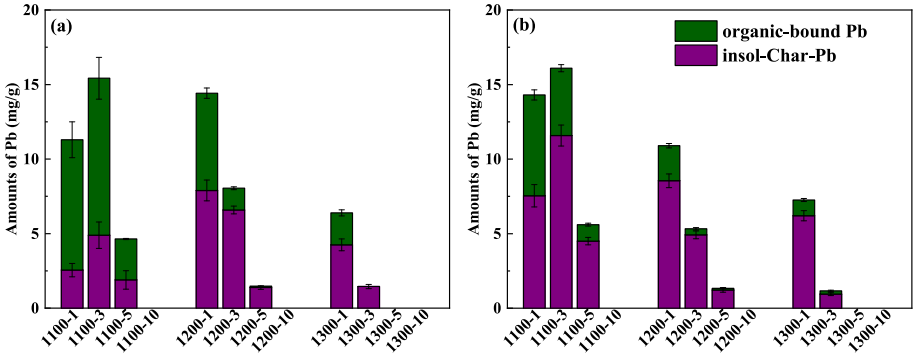

Fig. 6. Form distribution of Char-Pb retained by fulvic acid char: (a) $PbCl_2$, (b) PbO.

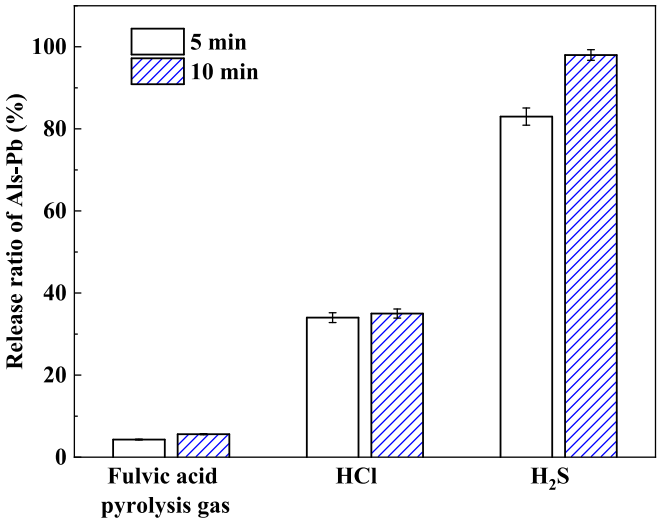

Fig. 7. Release ratio of Als-Pb under the action of volatiles at 1200 °C.

rapid reduction in Als-Pb content occurred at the same stage as the massive release of H_2S. At 1100 °C, the amount of H_2S released in the devolatilization of #1 coal was significantly lower than that for the other three coal types, while the proportion of Als-Pb in #1 coal was higher. Therefore, Als-Pb in #1 coal was not completely released. With the increase of temperature, the release rate and amount of H_2S increased, and the reaction rate between H_2S and Als-Pb accelerated. Therefore, the proportion of Als-Pb continuously declined until the complete release of Als-Pb at 1300 °C.

3.2.3. *Transformation paths of Pb during coal devolatilization*

The transformation paths of Pb in the coal devolatilization stage were established, as shown in Fig. 9. In raw coal, Pb existed in various forms, mainly carbonate- and oxide-bound form, sulfide-bound form, and residual form (Als-Pb). Carbonate- and oxide-bound and sulfide-bound Pb was thermally unstable and could be completely decomposed and released at 1100 °C. The release rate increased with an increase in temperature. Als-Pb was thermally stable, but was released under the action of H_2S generated during coal devolatilization. The release ratio of Als-Pb depended not only on the amount of H_2S and Als-Pb, but also on the reaction temperature. Pb released during the devolatilization of coal temporarily combined with char to form Char-Pb. Char-Pb was thermally unstable. In the late stage of devolatilization, the concentration of gas-phase Pb in the sample layer was low, and Char-Pb decomposed and was released, completely emitting this part of Pb to the gas phase.

The transformation of Pb during coal devolatilization not only causes a large proportion of Pb to be emitted at this stage but also determines the distribution of Pb in the char at the beginning of the combustion stage, and therefore affects the distribution of Pb in char combustion products. In the co-combustion of coal together with sludge, biomass, or other fuels [50], the devolatilization characteristics will most likely differ from the ones observed in this study, which will also affect the emission characteristics of Pb pollutants. The results on Pb transformation in the coal devolatilization and char combustion stages can provide guidance for predicting Pb emissions from coal combustion or co-combustion with different fuels under various conditions.

4. Conclusions

Dynamic release curves of Pb during the devolatilization of four types of coal at 1100–1300 ℃ were obtained. The release ratio of Pb first increased and then stabilized with time. At 1100 °C, Pb in #2, #3, and #4 coals was completely released, and the final release ratio of Pb in #1 coal was 87%. The increasing temperature promoted the release of Pb; thus, Pb in #1 coal was completely released at 1300 °C. The release ratio of Pb lagged behind that of coal devolatilization until it stabilized. The release ratios of Pb at the end of devolatilization of different coal types significantly differed, but all increased with increasing temperature: 42%–72% at 1100 °C, 65%–80% at 1200 °C, and 70%–92% at 1300 °C.

Pb was present in coal mainly in carbonate- and oxide-bound, sulfide-bound, and residual forms. The change in the distribution of Pb forms in the solid products during devolatilization suggested that each original form of Pb in coal was released. Arranged by thermal stability in ascending order, the forms of Pb are as follows: water-soluble and ion-exchangeable Pb < sulfide-bound Pb < carbonate- and oxide-bound Pb < organic-bound Pb < residual Pb. In solid devolatilization products, organic-bound Pb and residual Pb first increased and then decreased, indicating the transformation between different forms of Pb.

During coal devolatilization, the solid product char retained gaseous Pb as Char-Pb, which caused the increase in the proportion of organic-bound and residual Pb. Char-Pb first rapidly increased and then gradually decreased to zero. According to sequential chemical extraction results, Char-Pb can be divided into two forms: organic-bound Pb and insol-Char-Pb. Char-Pb formed from gaseous $PbCl_2$ and char was mainly in organic-bound form, whereas Char-Pb formed from gaseous PbO and char was mainly insol-Char-Pb. Char-Pb produced from coal was mainly insol-Char-Pb, and its thermal stability was higher than that of organic-bound Pb.

The original residual Pb in coal was mainly aluminosilicate (Als-Pb), which was released during devolatilization. Its release characteristics

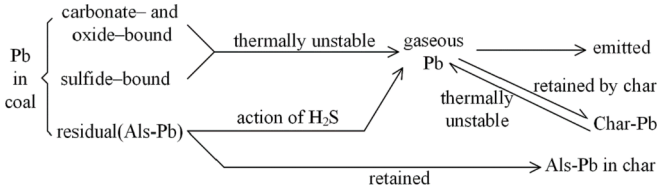

Fig. 9. Transformation paths of Pb during coal devolatilization.

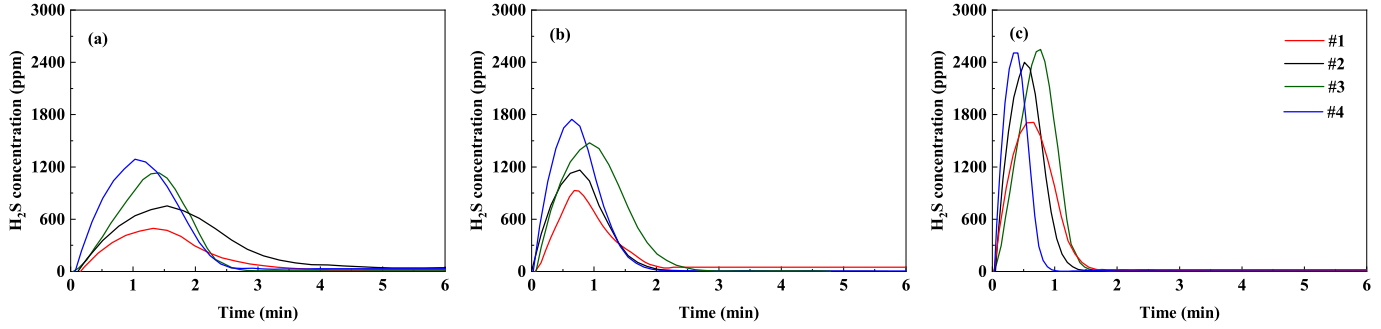

Fig. 8. Concentration of H_2S in gas products of coal devolatilization: (a) 1100 °C, (b) 1200 °C, (c) 1300 °C.

varied with coal type and temperature. Als-Pb in #2, #3, and #4 coals was completely released at 1100 °C, whereas in #1 coal, 13% and 7% of Als-Pb were present in solid products at 1100 and 1200 °C, respectively. H_2S generated during coal devolatilization was the main factor leading to the release of Als-Pb. The amount of H_2S produced in the devolatilization of #1 coal was significantly lower than those for the other three types of coal; therefore, some residual Pb existed stably at 1100 and 1200 °C.

The transformation paths of Pb in the devolatilization stage of coal were established, including the direct gas-phase release of different forms of Pb in coal and the reversible conversion between gaseous Pb and solid Char-Pb. The results can provide guidance for the study of Pb emission and control in different combustion processes.

CRediT authorship contribution statement

Guo-chang Song: Conceptualization, Methodology, Formal analysis, Investigation, Writing – original draft. **Wen-ting Xu:** Methodology, Validation, Writing – review & editing, Resources, Visualization. **Xing-yu Yang:** Methodology, Validation, Writing – review & editing. **Qiang Song:** Writing – review & editing, Supervision, Project administration, Funding acquisition.

Declaration of Competing Interest

The authors declare that they have no known competing financial interests or personal relationships that could have appeared to influence the work reported in this paper.

Data availability

Data will be made available on request.

Acknowledgements

This work was financially supported by the China National Key Research and Development Program (2022YFC3701503) and the Fundamental Research Funds for the Central Universities of China (2022ZFJH004).

Appendix A. Supplementary data

Supplementary data to this article can be found online at https://doi.org/10.1016/j.fuel.2023.127549.

References

[1] Saha D, Chatterjee D, Chakravarty S, Roychowdhury T. Investigation of environmental-concern trace elements in coal and their combustion residues from thermal power plants in eastern India. Nat Resour Res 2019;28:1505–20. https://doi.org/10.1007/s11053-019-09451-2.
[2] Finkelman RB. Potential health impacts of burning coal beds and waste banks. Int J Coal Geol 2004;59:19–24. https://doi.org/10.1016/j.coal.2003.11.002.
[3] Soltani N, Keshavarzi B, Moore F, Tavakol T, Lahijanzadeh AR, Jaafarzadeh N, et al. Ecological and human health hazards of heavy metals and polycyclic aromatic hydrocarbons (PAHs) in road dust of Isfahan metropolis. Iran Sci Total Environ 2015;505:712–23. https://doi.org/10.1016/j.scitotenv.2014.09.097.
[4] U.s.. Environmental Protection Agency. National emission standards for hazardous air pollutants from coal and oil–fired electric utility steam generating units and standards of performance for fossil–fuel–fired electric utility, industrial–commercial–institutional, and small industrial–commercial–institutional steam generating units. Fed Reg 2012;77(32):9487–8.
[5] Union E. Directive (EU) 2016/2284 of the European Parliament and of the Council of 14 December 2016 on the reduction of national emissions of certain atmospheric pollutants, amending Directive 2003/35/EC and repealing Directive 2001/81/EC. Off J Eur Union 2016;344:1–31.
[6] Wang T, Lou YB, Jiang SC, Wang JW, Zhang YS, Pan WP. Distribution characteristics and environmental risk assessment of trace elements in desulfurization sludge from coal-fired power plants. Fuel 2022;314:122771. https://doi.org/10.1016/j.fuel.2021.122771.
[7] Zhao SL, Duan YF, Wang CP, Liu M, Lu JH, Tan HZ, et al. Migration behavior of trace elements at a coal–fired power plant with different boiler loads. Energy Fuels 2017;31:747–54. https://doi.org/10.1021/acs.energyfuels.6b02393.
[8] Zhang ZP, Li YZ, Zhang XY, Zhang HW, Wang L. Review of hazardous materials in condensable particulate matter. Fuel Process Technol 2021;220:106892. https://doi.org/10.1016/j.fuproc.2021.106892.
[9] Seames WS, Wendt JOL. Partitioning of arsenic, selenium, and cadmium during the combustion of Pittsburgh and Illinois #6 coals in a self–sustained combustor. Fuel Process Technol 2000;63:179–96. https://doi.org/10.1016/S0378-3820(99)00096-X.
[10] Liu RQ, Zhang XL, Wang JW, Wang TJ, Xie JF. Transformation behaviors of lead during thermal treatment of Heidaigou coal. Energy Sources, Part A 2014;36:1366–71. https://doi.org/10.1080/15567036.2011.553660.
[11] Wang JW, Zhang YS, Wang T, Xu H, Pan WP. Effect of modified fly ash injection on As, Se, and Pb emissions in coal–fired power plant. Chem Eng J 2020;380:122561. https://doi.org/10.1016/j.cej.2019.122561.
[12] Xu WT, Song GC, Song Q, Yao Q. Study on the mechanism of lead release from ash under the action of high-temperature flue gas. Fuel Process Technol 2022;227:107089. https://doi.org/10.1016/j.fuproc.2021.107089.
[13] Verma SK, Masto RE, Gautam S, Choudhury DP, Ram LC, Maiti SK, et al. Investigations on PAHs and trace elements in coal and its combustion residues from a power plant. Fuel 2015;162:138–47. https://doi.org/10.1016/j.fuel.2015.09.005.
[14] Ji P, Song GC, Xu WT, Song Q. Transformation characteristics of arsenic and lead during coal combustion. Energy Fuels 2019;33:9280–8. https://doi.org/10.1021/acs.energyfuels.9b02189.
[15] Xue ZY, Dong L, Zhong ZP, Lai XD, Huang YJ. Capture effect of Pb, Zn, Cd and Cr by intercalation–exfoliation modified montmorillonite during coal combustion. Fuel 2021;290:119980. https://doi.org/10.1016/j.fuel.2020.119980.
[16] Wang J, Tomita A. A chemistry on the volatility of some trace elements during coal combustion and pyrolysis. Energy Fuels 2003;17:954–60. https://doi.org/10.1021/ef020251o.
[17] G.C. Song, W.T. Xu, Q. Song. Prediction model for lead release during coal combustion based on ash fusion temperature. Proc. CSEE, in press. doi: 10.13334/j.0258-8013.pcsee.212963.
[18] Zhao SL, Duan YF, Lu JC, Gupta R, Pudasainee D, Liu S, et al. Chemical speciation and leaching characteristics of hazardous trace elements in coal and fly ash from coal–fired power plants. Fuel 2018;232:463–9. https://doi.org/10.1016/j.fuel.2018.05.135.
[19] Finkelman RB, Palmer CA, Wang PP. Quantification of the modes of occurrence of 42 elements in coal. Int J Coal Geol 2018;185:138–60. https://doi.org/10.1016/j.coal.2017.09.005.
[20] Zhang SR, Jiang XG, Lv GJ, Nixiang A, Jin YQ, Yan JH, et al. Effect of chlorine, sulfur, moisture and ash content on the partitioning of As, Cr, Cu, Mn, Ni and Pb during bituminous coal and pickling sludge co–combustion. Fuel 2019;239:601–10. https://doi.org/10.1016/j.fuel.2018.11.061.
[21] Uberoi M, Shadman F. Sorbents for removal of lead compounds from hot flue gases. AICHE J 1990;36:307–9. https://doi.org/10.1002/aic.690360220.
[22] Yu MZ, Huang YJ, Xia WQ, Zhu ZC, Fan CH, Liu CQ, et al. $PbCl_2$ capture by kaolin and metakaolin under different influencing factors of thermal treatment. Energy Fuels 2020;34:2284–92. https://doi.org/10.1021/acs.energyfuels.9b03217.
[23] Wang SJ, He PJ, Shao LM, Zhang H. Multifunctional effect of Al_2O_3, SiO_2 and CaO on the volatilization of PbO and $PbCl_2$ during waste thermal treatment. Chemosphere 2016;161:242–50. https://doi.org/10.1016/j.chemosphere.2016.07.020.
[24] Bartoňová L, Raclavská H, Čech B, Kucbel M. Behavior of Pb during coal combustion: an overview. Sustainability 2019;11:6061. https://doi.org/10.3390/su11216061.
[25] Huang QX, Cai X, Alhadj Mallah MM, Chi Y, Yan JH. Effect of $HCl/SO_2/NH_3/O_2$ and mineral sorbents on the partitioning behaviour of heavy metals during the thermal treatment of solid wastes. Environ Technol 2015;36:3043–9. https://doi.org/10.1080/09593330.2014.963693.
[26] Jerzak W. Equilibrium calculations of As, Pb, and Hg speciations during coal combustion in atmospheres $21O_2/79N_2$ and $30O_2/70CO_2$. Energy Sources, Part A 2016;38:2679–86. https://doi.org/10.1080/15567036.2015.1110643.
[27] Chiang KY, Wang KS, Lin FL, Chu WT. Chloride effects on the speciation and partitioning of heavy metal during the municipal solid waste incineration process. Sci Total Environ 1997;203:129–40. https://doi.org/10.1016/S0048-9697(97)00140-X.
[28] Zhang AJ, Liu J, Yang YJ, Yu YN, Zhang JY. Reaction chemistry of $PbSO_4$ formation over Al_2O_3 sorbent. Fuel 2022;310:122407. https://doi.org/10.1016/j.fuel.2021.122407.
[29] Abdel-Rehim AM. Thermal and XRD analysis of Egyptian galena. J Therm Anal Calorim 2006;86:393–401. https://doi.org/10.1007/s10973-005-6785-6.
[30] Zhou H, Li Y, Li N, Qiu RC, Cen KF. Conversions of fuel-N to NO and N_2O during devolatilization and char combustion stages of a single coal particle under oxy-fuel fluidized bed conditions. J Energy Inst 2019;92:351–63. https://doi.org/10.1016/j.joei.2018.01.001.
[31] Zhao HB, Song Q, Wu XY, Yao Q. Study on the transformation of inherent potassium during the fast-pyrolysis process of rice straw. Energy Fuels 2015;29:6404–11. https://doi.org/10.1021/acs.energyfuels.5b00851.
[32] Viljanen J, Zhao HB, Zhang ZH, Toivonen J, Alwahabi ZT. Real-time release of Na, K and Ca during thermal conversion of biomass using quantitative microwave-assisted laser-induced breakdown spectroscopy. Spectrochim Acta, Part B 2018;149:76–83. https://doi.org/10.1016/j.sab.2018.07.022.

[33] Hedayati A, Sefidari H, Boman C, Skoglund N, Kienzl N, Ohman M. Ash transformation during single-pellet gasification of agricultural biomass with focus on potassium and phosphorus. Fuel Process Technol 2021;217:106805. https://doi.org/10.1016/j.fuproc.2021.106805.
[34] Strugnell B, Patrick JW. Rapid hydropyrolysis studies on coal and maceral concentrates. Fuel 1996;75:300–6. https://doi.org/10.1016/0016-2361(95)00241-3.
[35] Xu RS, Zhang JL, Wang GW, Zuo HB, Liu ZJ, Jiao KX, et al. Devolatilization characteristics and kinetic analysis of lump coal from China COREX3000 under high temperature. Metall Mater Trans B 2016;47:2535–48. https://doi.org/10.1007/s11663-016-0708-8.
[36] Sugawara K, Tozuka Y, Sholes MA, Kamoshita T, Sugawara T, Sholes M. Dynamic behaviour of sulfur forms in rapid pyrolysis of density-separated coals. Fuel 1994;73:1224–8. https://doi.org/10.1016/0016-2361(94)90264-X.
[37] Song GC, Xu WT, Yang XY, Song Q. Coupling effects of mineral components on arsenic transformation during coal combustion. J Hazard Mater 2022;435:129040. https://doi.org/10.1016/j.jhazmat.2022.129040.
[38] Zhang YQ, Zhu JL, Wang XH, Zhang XW, Zhou SX, Liang P. Simulation of large coal particles pyrolysis by circulating ash heat carrier toward the axial dimension of the moving bed. Fuel Process Technol 2016;154:227–34. https://doi.org/10.1016/j.fuproc.2016.08.037.
[39] Song GC, Xu WT, Ji P, Song Q. Study on the transformation of arsenic and lead in pyrite during thermal conversion. Energy Fuels 2019;33:8463–70. https://doi.org/10.1021/acs.energyfuels.9b02028.
[40] Song GC, Xu WT, Liu K, Song Q. Transformation of selenium during coal thermal conversion: Effects of atmosphere and inorganic content. Fuel Process Technol 2020;205:106446. https://doi.org/10.1016/j.fuproc.2020.106446.
[41] Yu JF, Zhang XZ, Jin BS, Chen JX, Huang YJ, Wang ZF. Silica aluminum xerogel-based sorbent for removal of volatilized $PbCl_2$ during the incineration: Improvement on mass-transfer limitations via high porosity. Sci Total Environ 2021;782:146925. https://doi.org/10.1016/j.scitotenv.2021.146925.
[42] Xu WT, Song Q, Zhao HB, Zhuo JK, Yao Q. Study on the capture of gaseous KCl by cellulose char. Energy Fuels 2019;33:362–8. https://doi.org/10.1021/acs.energyfuels.8b03533.
[43] Ngo TNLT, Chiang KY. The migration, transformation and control of trace metals during the gasification of rice straw. Chemosphere 2020;260:127540. https://doi.org/10.1016/j.chemosphere.2020.127540.
[44] Durlak SK, Biswas P, Shi JC. Equilibrium analysis of the effect of temperature, moisture and sodium content on heavy metal emissions from municipal solid waste incinerators. J Hazard Mater 1997;56:1–20. https://doi.org/10.1016/S0304-3894(97)00002-2.
[45] Shah P, Strezov V, Nelson PF. X-Ray Absorption Near Edge Structure Spectrometry study of nickel and lead speciation in coals and coal combustion products. Energy Fuels 2009;23:1518–25. https://doi.org/10.1021/ef800824d.
[46] Gong GQ, Yuan X, Zhang YJ, Li YJ, Liu WX, Wang M, et al. Characterization of coal-based fulvic acid and the construction of a fulvic acid molecular model. RSC Adv 2020;10:5468–77. https://doi.org/10.1039/C9RA09907G.
[47] Zou C, Ma C, Zhao JX, Shi RM, Li XM. Characterization and non-isothermal kinetics of Shenmu bituminous coal devolatilization by TG-MS. J Anal Appl Pyrolysis 2017;127:309–20. https://doi.org/10.1016/j.jaap.2017.07.020.
[48] Rio S, Verwilghen C, Ramaroson J, Nzihou A, Sharrock P. Heavy metal vaporization and abatement during thermal treatment of modified wastes. J Hazard Mater 2007;148:521–8. https://doi.org/10.1016/j.jhazmat.2007.03.009.
[49] Bohnstein MV, Yildiz C, Frigge L, Strhle J, Epple B. Simulation study of the formation of corrosive gases in coal combustion in an entrained flow reactor. Energies 2020;13:4523. https://doi.org/10.3390/en13174523.
[50] Zhao ZH, Wang RK, Wu JH, Yin QQ, Wang CB. Bottom ash characteristics and pollutant emission during the cocombustion of pulverized coal with high mass-percentage sewage sludge. Energy 2019;171:809–18. https://doi.org/10.1016/j.fuproc.2020.106665.